

# Comparing the sugar profiles and primary structures of alkali-extracted water-soluble polysaccharides in cell wall between the yeast and mycelial phases from *Tremella fuciformis*

Hanyu Zhu<sup>1</sup>, Yuan Yuan<sup>1</sup>, Juan Liu<sup>1</sup>,  
Liesheng Zheng<sup>2</sup>, Ligu Chen<sup>2</sup>, and Aimin Ma<sup>1,3\*</sup>

<sup>1</sup>College of Food Science and Technology, Huazhong Agricultural University, Wuhan 430070, P. R. China

<sup>2</sup>College of Plant Science and Technology, Huazhong Agricultural University, Wuhan 430070, P. R. China

<sup>3</sup>Key Laboratory of Agro-Microbial Resources and Utilization, Ministry of Agriculture, Huazhong Agricultural University, Wuhan 430070, P. R. China

(Received Oct 27, 2015 / Revised Mar 4, 2016 / Accepted Mar 18, 2016)

To gain insights into dimorphism, cell wall polysaccharides from *Tremella fuciformis* strains were obtained from alkali-extracted water-soluble fractions PTF-M38 (from the mycelial form), PTF-Y3 and PTF-Y8 (from the yeast form) of *T. fuciformis* strains were used to gain some insights into dimorphism study. Their chemical properties and structural features were investigated using gel permeation chromatography, gas chromatography, UV and IR spectrophotometry and Congo red binding reactions. The results indicated that the backbones of PTF-M38, PTF-Y3 and PTF-Y8 were configured with  $\alpha$ -linkages with average molecular weights of 1.24, 1.08, and 1.19 kDa, respectively. PTF-M38 was mainly composed of xylose, mannose, glucose, and galactose in a ratio of 1:1.47:0.48:0.34, while PTF-Y3 and PTF-Y8 were mainly composed of xylose, mannose and glucose in a ratio of 1:1.65:4.06 and 1:1.21:0.44, respectively. The sugar profiles of PTF-M38, PTF-Y3 and PTF-Y8 were also established for further comparison. These profiles showed that all three polysaccharides contained the same sugars but in different ratios, and the carbon sources (xylose, mannose, glucose, and galactose) affected the sugar ratios within the polysaccharides.

**Keywords:** *Tremella fuciformis*, cell wall polysaccharide, structure analysis, sugar profile, fungal dimorphism

## Introduction

Dimorphism is a morphological transition between a unicellular yeast phase and a multicellular filamentous phase that shows peculiar characteristic in fungi (Rappleye and Goldman, 2006). Dimorphic change is reversible and depends upon the

environment to which the fungi are exposed (Georgopapadakou and Walsh, 1994; Ghormade and Deshpande, 2000). Many factors trigger this intriguing morphological transition, such as pH, temperature, limitations in nutrients, chemical molecules, and intracellular signal transduction pathways (Maresca and Kobayashi, 1989; Liu *et al.*, 2008; Nadal *et al.*, 2008; Chauhan *et al.*, 2011). Regarding pathogenetic dimorphic fungi, it has long been believed that dimorphism is necessary for pathogenicity, but the mechanism that regulates this switch has remained a mystery (Nemecek *et al.*, 2006). Interestingly, many studies have observed that the carbohydrates composition in the cell wall during dimorphic transition were altered, thus opening up a perspective for studying the relationship between cell wall composition and dimorphism (Klein and Tebbets, 2007; Klis *et al.*, 2007; Puccia *et al.*, 2011).

There is ample evidence suggesting that cell wall carbohydrates from the yeast form of dimorphic fungi are fully comparable to those from the mycelial form. As the published data have shown, the concentrations of fucose- and galactose-containing polymers are higher in the mycelial form of the cell wall of *Mucor rouxii* than the yeast form (Dow *et al.*, 1983). In the case of *Candida albicans*, when grown into the mycelial form, chitin is preferentially deposited in the hyphal tip (Braun and Calderone, 1978; Sietsma and Wessels, 1994). In *Blastomyces dermatitidis*, the transition from mycelium to yeast is accompanied by a considerable increase in the level of  $\alpha$ -1,3-glucan and a decrease in the  $\beta$ -1,3-glucan contents of the cell wall (San-Blas *et al.*, 1984). In addition, the level of  $\alpha$ -1,3-glucan,  $\beta$ -1,3-glucan, and chitin in the hyphal wall are totally different from the levels in the yeast wall (Kanetsuna and Carbonell, 1971). Studies have found that the level of  $\alpha$ -1,3-glucan in the cell wall polysaccharides was correlated with the pathogenicity of several dimorphic fungi, thus indicating its great importance (Hogan and Klein, 1994). The reason why  $\alpha$ -1,3-glucan contributes to pathogenesis might be it conceals immunostimulatory  $\beta$ -glucans from being detected by the host (Rappleye *et al.*, 2007). Comparisons of the carbohydrate composition and structure characterization between the cell walls of the mycelial and yeast phases from some fungi have already been undertaken to gain some insights into dimorphic change (Ahrazem *et al.*, 2003; Mysyakina *et al.*, 2012).

*Tremella fuciformis*, an edible basidiomycetous jelly mushroom, has been favored by Chinese people for centuries. *T. fuciformis* has the capacity to grow in either the yeast or mycelial form and this type of cell differentiation is a reversible process (Liu *et al.*, 2007). Previous studies have focused

\*For correspondence. E-mail: aiminma@mail.hzau.edu.cn; Tel.: +86-27-87282111

mainly on how environmental factors triggered dimorphic transition in *T. fuciformis* (Hou *et al.*, 2011). However, few researches on dimorphic change of *T. fuciformis* have been carried out, but being a nonpathogenetic dimorphic fungus, it is worthy of consideration.

The present study aims to compare the alkali-extracted water-soluble polysaccharides fractions from the cell walls of the yeast and mycelial forms of *T. fuciformis*. We purified the polysaccharides fractions and characterized their primary structures. The influence of carbon source on the sugar profile was also established in order to further evaluate any differences.

## Materials and Methods

### Strains and growth conditions

A dikaryotic strain of *T. fuciformis* M38 (mycelial form) and two parental monokaryotic strains Y3 and Y8 (yeast form), were kept at the Laboratory of Food Microbiology, Huazhong Agricultural University and maintained at 25°C on potato dextrose agar (Difco) slants. The liquid medium designed for strain culturing contained the following components per liter of distilled water: glucose, 20 g; (NH<sub>4</sub>)<sub>2</sub>SO<sub>4</sub>, 1.32 g; MgSO<sub>4</sub>·7H<sub>2</sub>O, 0.25 g; KH<sub>2</sub>PO<sub>4</sub>·3H<sub>2</sub>O, 0.5 g; vitamin B<sub>1</sub>, 0.2 mg; ZnSO<sub>4</sub>·7H<sub>2</sub>O, 2 mg; and CaCl<sub>2</sub>·2H<sub>2</sub>O, 0.5 g. Strains were incubated at 25°C using an orbital shaker (Fuma) at 150 rpm for 3–5 days.

### Extraction and purification of alkali-extracted water-soluble cell wall polysaccharide fractions

The cell wall materials were extracted using the method described by Leung *et al.* (1997). The cell wall material (8 g) was then repeatedly extracted to obtain polysaccharide fractions using 1 M NaOH (300 ml) treatment for 20 h at room temperature (Ahrazem *et al.*, 2000). After centrifugation at 10,000 × g, the supernatants were combined and 1 M HCl was added to neutralize. The concentrated supernatants with 3 volumes of 95% ethanol were maintained at 4°C overnight in order to facilitate the precipitation of the polysaccharides. The precipitates were then dissolved in distilled water and recentrifuged followed by dialysis. Finally, the crude alkali-extracted water-soluble cell wall polysaccharides were lyophilized by freeze-drying.

The crude polysaccharides (600 mg), dissolved in 10 ml distilled water, were centrifuged at 10,000 × g for 10 min. The supernatants were then collected, and loaded onto a DEAE-52 cellulose column (1.5 cm × 20 cm; Sigma) eluted with 0.1 M NaCl at a rate of 0.4 ml/min twice. The eluted fractions were collected using an automated step-by-step fraction collector and measured at 675 nm by the anthrone-sulfuric acid colorimetric method for each fraction. Fractions that corresponded to the high absorbance material containing purified polysaccharides fractions were collected and lyophilized.

### Measurements of carbohydrate, uronic acid, and protein contents

The carbohydrate content was measured by the phenol-sulfuric acid method using glucose as a standard (Dubois *et al.*, 1956). The uronic acid content was determined by the carbazole reaction using glucuronic acid as a standard (Blumen-

krantz and Asboe-Hansen, 1973). The protein content was measured by the Coomassie brilliant blue G-250 methods (Bradford 1976) using bovine serum albumin as a standard.

### Estimation of molecular weight

The molecular weights of the polysaccharide fractions from each strain were determined by gel permeation chromatography, using a PL aquagel-OH MIXED column (30 cm × 0.75 cm; Agilent). The sample (50 µl) was monitored with a RID-10A Refractive Index Detector (Shimadzu), using a mixture of 0.1 M NaAc and 0.2 M HAc as the eluent, at a flow rate of 1 ml/min. A standard curve with the elution volume plotted against the logarithm of molecular weight, was constructed using the Dextran T standards (MW: 10, 40, 70, 500, and 2,000 kDa).

### Determination of monosaccharide composition

Gas chromatography (GC) was used for monosaccharide identification and quantification (Li *et al.*, 2013). The sample (10 mg) was hydrolyzed with 2 M trifluoroacetic acid (2 ml) at 110°C in a sealed tube for 2 h, followed by drying to neutralize the pH of the mixture through evaporation. Acetylation was performed with 10 mg hydroxylamine hydrochloride and 0.5 ml pyridine for 30 min at 90°C. Acetic anhydride (0.5 ml) was subsequently added for a further 30 min heating, then the alditol acetate derivatives samples were analyzed on a gas chromatography (Agilent 6890N GC; flame ionization detector, Agilent) fitted with an HP-5 capillary column (30 m × 0.32 mm × 0.25 µm). The column and injector temperature were 250 and 270°C, respectively. The carrier gas was nitrogen (50 ml/min) with an injected volume of 2.5 µl.

### Identification of conformational structure

For identifying the conformational structures, the method of Kraus *et al.* (1992) was followed with minor modifications. Each 50 µl polysaccharide sample (0.5 mg/ml) was mixed with 350 µl Congo red solution (0.02 mg/ml), NaOH was added to each mixture at 10 different final concentrations (0.05 M – 0.5 M) to study the dependence of the λ<sub>max</sub> of Congo red-glucan complex on the concentration of NaOH. The absorption spectrum of the Congo red-glucan complex at each NaOH concentration was scanned from 400 nm to 600 nm and λ<sub>max</sub> was determined with an ultraviolet-visible spectrophotometer (UV-1700; Shimadzu).

### Analysis of UV and IR

UV-visible spectra were performed on an ultraviolet-visible spectrophotometer (UV-1700; Shimadzu) at 25°C in the range of 200–400 nm, using a quartz cell with a 1 cm path length. IR spectra were recorded in the frequency range of 600–4000 cm<sup>-1</sup> (Nexus 470; Nicolet). The dried polysaccharide samples (2.0 mg) were mixed with KBr powder (spectroscopic grade), grounded then crushed.

### Effect of carbon sources on sugar profiles of polysaccharides

The liquid media for establishment of the sugar profiles were the same as that used for culturing the strains of *T. fuci-*

**Table 1.** Chemical composition of PTF-M38, PTF-Y3 and PTF-Y8

Chemical composition (% w/w)	PTF-M38	PTF-Y3	PTF-Y8
Total sugar	78.09 ± 1.12 <sup>a</sup>	92.64 ± 0.86 <sup>a</sup>	88.12 ± 1.02 <sup>a</sup>
Uronic acid	13.99 ± 0.24 <sup>a</sup>	1.82 ± 0.57 <sup>b</sup>	3.03 ± 1.15 <sup>b</sup>
Protein	0.52 ± 0.41 <sup>a</sup>	0.16 ± 0.88 <sup>a</sup>	0.33 ± 0.98 <sup>ab</sup>

All values are means ± SD (n=3); different superscript letters in the same row indicate significant differences between mean values of different samples at  $P < 0.05$ .

*formis* using carbon sources of xylose, mannose, glucose and galactose with incubation at 25°C for 3–5 days. The strains were collected then the cell wall polysaccharides extracted as described earlier. The chemical composition of the purified polysaccharide fractions was determined by gas chromatography following the method described earlier.

## Results

### Molecular weight of PTF-M38, PTF-Y3, and PTF-Y8

The water-soluble cell wall polysaccharide fractions extracted by alkali from the mycelial form was termed PTF-M38 and from the yeast form was named as PTF-Y3 and PTF-Y8. A calibration curve was obtained by using various Dextran T-

series standards of known molecular weights. Based on the calibration curve, the average molecular weights of PTF-M38, PTF-Y3, and PTF-Y8 were calculated to be 1.24, 1.08, and 1.19 kDa, respectively (data not shown).

### Carbohydrate, uronic acid, and protein contents of PTF-M38, PTF-Y3, and PTF-Y8

The contents of total sugar, uronic acid, and protein of each polysaccharide fraction are summarized in Table 1. For the PTF-M38, PTF-Y3, and PTF-Y8, the total sugar contents 78.09%, 92.64%, and 88.12%, respectively; the contents of total uronic acid were 13.99%, 1.82%, and 3.03%, respectively; the protein contents were 0.52%, 0.16%, and 0.33%, respectively. The total sugar and protein contents of PTF-M38, PTF-Y3, and PTF-Y8 were similar, but the uronic acid contents were dissimilar.

### Monosaccharide composition of PTF-M38, PTF-Y3, and PTF-Y8

From the peak areas obtained by GC analysis (Fig. 1), the polysaccharides from M38 were composed mainly of xylose, mannose, glucose, and galactose in the ratio of 1:1.47:0.48:0.34 while PTF-Y3 and PTF-Y8 were composed mainly of xylose, mannose and glucose in the ratio of 1:1.65:4.06 and 1:1.21:0.44, respectively. Galactose was hardly examined in PTF-Y3 and PTF-Y8.

### Secondary structure of PTF-M38, PTF-Y3, and PTF-Y8

Glucan can bind with Congo red dye to form Congo red-glucan complex. The  $\lambda_{\max}$  value of the complex is affected by the structure of the glucan as the concentration of NaOH

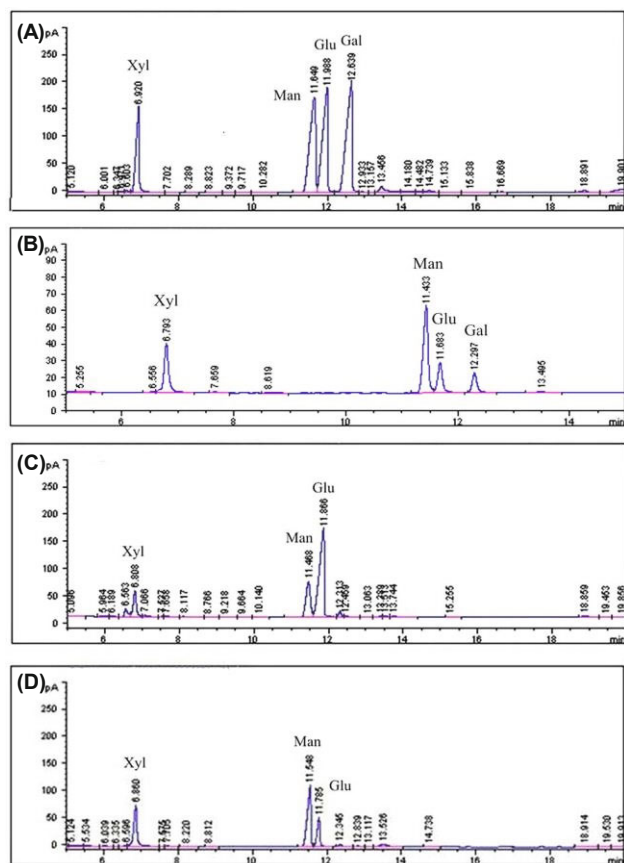


**Fig. 1.** GC traces of cell wall polysaccharides extracted from *T. ficiformis*. (A) Standard monosaccharide; (B) PTF-M38; (C) PTF-Y3; (D) PTF-Y8. Monosaccharide: xylose (Xyl), mannose (Man), glucose (Glu), and galactose (Gal).

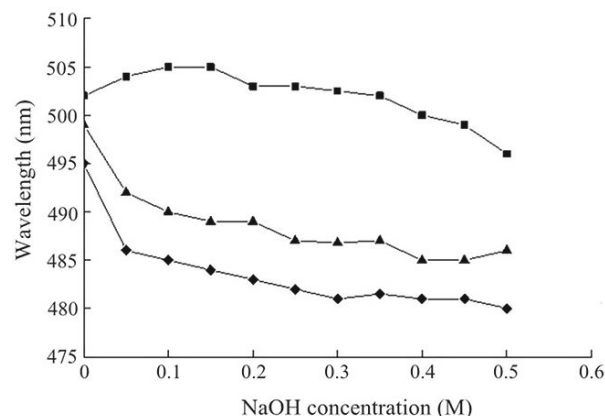


**Fig. 2.** Helix-coil transition analysis of PTF-M38. -■-,  $\beta$ -glucan; -◆-, distilled water; -▲-, PTF-M38.

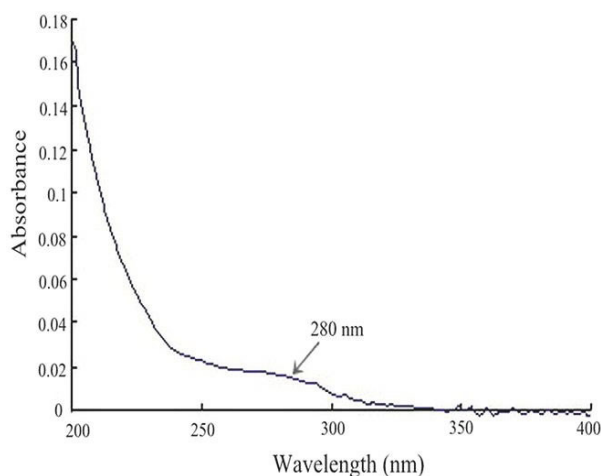


**Fig. 3.** UV spectrum of PTF-M38.

increases.  $\beta$ -1,3-Glucan, exhibits a triple-helical conformation, when bound to Congo red dye, value of the  $\lambda_{\max}$  of the complex varying with the concentration of NaOH. From the results, shifts in the absorption maximum of Congo red in the presence of PTF-M38, PTF-Y3 and PTF-Y8 were similar. As shown in Fig. 2 (PTF-M38 only), an increase in NaOH concentration results in a much higher  $\lambda_{\max}$  value for the Congo red dye and  $\beta$ -1,3-glucan complex (as the control) than that of the complex of Congo red dye and each of the extracted polysaccharides. It can also be observed that the  $\lambda_{\max}$  value of the complex of Congo red dye and extracted polysaccharide fractions were similar to those of Congo red only. It can thus be speculated that the backbone of PTF-M38, PTF-Y3, and PTF-Y8 were configured with  $\alpha$ -linkages.

#### UV and IR analysis of PTF-M38, PTF-Y3, and PTF-Y8

The UV spectra of PTF-M38, PTF-Y3, and PTF-Y8 showed great similarity. As seen from the absorption curve of PTF-M38 (Fig. 3), there was no absorption at 260 nm in the UV spectrum, indicating the absence of nucleic acid. Meanwhile, it was found that the weak peaks at 280 nm could be attributed to the absorption of proteins, which agreed with the results shown earlier on protein content.

The main IR absorption peaks of PTF-M38, PTF-Y3, and

PTF-Y8 are shown in Table 2. The results exhibited an IR absorption spectrum characteristic of a polysaccharide, with bands in the region of 3500–3200  $\text{cm}^{-1}$  (O-H), 3000–2800  $\text{cm}^{-1}$  (C-H) and 1400–1200  $\text{cm}^{-1}$  (C-H). The bands in the region of 1740–1680  $\text{cm}^{-1}$  were due to the C=O stretching vibration, suggesting the presence of uronic acid. The bands in the region of 1150–1060  $\text{cm}^{-1}$  and near 960  $\text{cm}^{-1}$  were due to pyran glycosyl. In addition, bands near 840  $\text{cm}^{-1}$  showed the presence of the  $\alpha$ -configuration glycosidic bond.

#### Establishment of sugar profile

Xylose, mannose, glucose, and galactose were adopted as the carbon sources. The results (Fig. 4) showed that the monosaccharide composition of PTF-M38, PTF-Y3, and PTF-Y8 were similar but exhibited different ratios. The sugar ratio of PTF-M38, PTF-Y3, and PTF-Y8 also varied with the strains and with the carbon sources.

#### Discussion

It is generally considered that the shape of a fungal cell is determined by the form of its wall. Bearing this concept in mind, changes in the cell wall structure and biosynthesis, or changes in the arrangement of the cell wall composition should accompany morphogenetic change in dimorphic fungi (San-Blas *et al.*, 1984). The fungal cell wall polysaccharides, significant components of the cell wall, have been stressed to study the evolutionary history of fungi and the classification of filamentous fungi at the genus or subgenus level (Bartnicki-García, 1987; Leal and Bernabé, 1998). Many polysaccharides in the fungal cell wall play roles in morphological change and, consequently, are thought to be related to the phenomenon of dimorphism (San-Blas *et al.*, 1984; Holbrook and Rappleye, 2008; Klis *et al.*, 2007; Dos Reis Almeida *et al.*, 2014).

Therefore, it is highly important to determine the structural differences between polysaccharides from both yeast and mycelial cell walls. Polysaccharides have the highest capacity for carrying biological information and differ greatly in their chemical composition, molecular weight, conformation, glycosidic linkage, and degree of branching, etc. (Lee *et al.*, 2010). From the results in the present study, the structural differences between PTF-M38, PTF-Y3, and PTF-Y8 are in their uronic acid contents, monosaccharide composition, and sugar

**Table 2.** IR analysis of PTF-M38, PTF-Y3, and PTF-Y8

Absorbance peak ( $\text{cm}^{-1}$ )			Vibration	Functional Group
PTF-M38	PTF-Y3	PTF-Y8		
3439.02	3447.85	3439.02	O-H stretching vibration, N-H stretching vibration	-OH, -NH <sub>2</sub> , >NH
2882.45	2882.45	2873.62	C-H stretching vibration	-CH <sub>2</sub>
1650.06	1645.64	1645.64	C=O stretching vibration, N-H deformation vibration	C=O (-COOH), -CONH
1468.96	1468.96	1464.54		
1345.28	1340.86	1340.86		
1283.44	1279.02	1283.44	C-O stretching vibration, C-H deformation vibration	C-O, -CH <sub>2</sub> (-COOH)
1234.85	1239.26	1239.26		
1102.33	1115.58	1115.58	C-O-C stretching vibration	C-O-C
952.15	956.56	965.40	terminal methyne rocking vibration	pyranoid ring
837.30	837.30	841.72	$\alpha$ -terminal group C-H deformation vibration	pyranoid ring

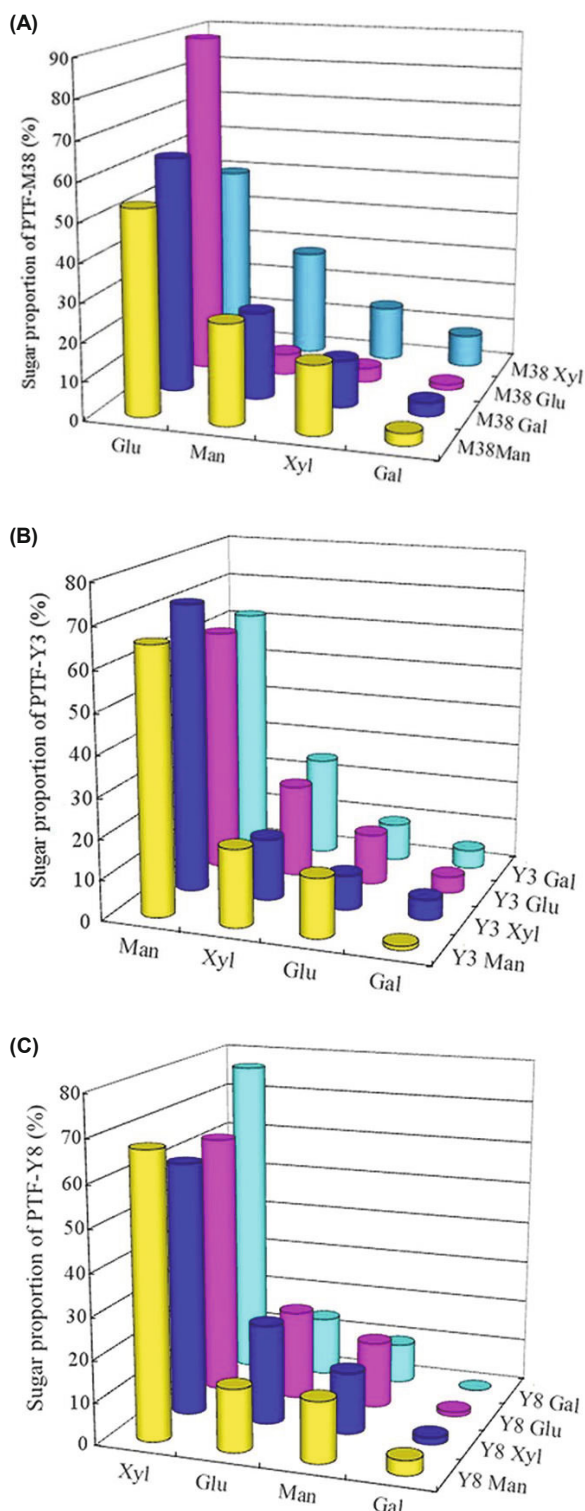


**Fig. 4.** Sugar profiles of different polysaccharides produced by *T. fuciformis*. (A) M38; (B) Y3; (C) Y8. x axis: carbon sources; y axis: monosaccharide contents; z axis: sugar proportion of cell wall polysaccharides. Carbon sources: xylose (Xyl), mannose (Man), glucose (Glu), and galactose (Gal).

profiles. First, the total sugar and protein contents of PTF-M38, PTF-Y3, and PTF-Y8 are similar, but the uronic acid

contents varied. Many biologically important polysaccharides contain uronic acid within their repeating units (Garron and Cygler, 2010). The different uronic acid contents in the cell wall could result in various polysaccharides structures and biological functions, which may contribute to the morphological transition. Second, regarding the monosaccharide composition (Fig. 1) of PTF-M38, PTF-Y3, and PTF-Y8, it is apparent that galactose is specifically presented in the hyphal wall. The same case also happens in the *Benjaminiella poitrasii* cell wall as the mannose content in the yeast phase is much higher than in the mycelial phase (Ghormade and Deshpande, 2000). Thus we can speculate that some monosaccharides may play important roles in the morphological change during dimorphism. Finally, the sugar ratios of PTF-M38, PTF-Y3 and PTF-Y8 varied both with strain and carbon source (Fig. 4). The sugar profiles indicated that their relationship with the strains is not static and depends on the environment to which the organisms are exposed. It appears that the sugar profiles of polysaccharides probably represents an averaging of the different types of polymers produced in these systems and the relationship between strains and environmental factors (Khondkar *et al.*, 2002). From the sugar profiles of PTF-M38, PTF-Y3, and PTF-Y8, these polysaccharide fractions exhibit differences in their monosaccharide composition, which further influences their cell wall structures.

In conclusion, the aim of the present study was to ascertain whether polysaccharides in the *T. fuciformis* cell wall differed between the mycelial and yeast forms, a fact that might have dimorphic relevance. From the results, the chemical properties and structural characteristics of PTF-M38, PTF-Y3, and PTF-Y8 differ in many aspects: uronic acid contents, monosaccharide composition, and sugar profiles. In addition, the chemical compositions of cell wall polysaccharides are changeable triggered by environmental factors such as carbon sources which further influence their cell wall structure. More systematical work to compare the mycelial and yeast cell walls of dimorphic fungi is necessary and warrants further study.

## Acknowledgements

This work was supported by grants from the National Natural Science Foundation of China (NSFC) (No. 30972072 and No. 31572182) to Aimin Ma.

## References

- Ahrazem, O., Gómez-Miranda, B., Prieto, A., Bernabé, M., and Leal, J.A. 2000. Heterogeneity of the genus *Myrothecium* as revealed by cell wall polysaccharides. *Arch. Microbiol.* **173**, 296–302.
- Ahrazem, O., Prieto, A., San-Blas, G., Leal, J.A., Jimenez-Barbero, J., and Bernabe, M. 2003. Structural differences between the alkali-extracted water-soluble cell wall polysaccharides from mycelial and yeast phases of the pathogenic dimorphic fungus *Paracoccidioides brasiliensis*. *Glycobiology* **13**, 743–747.
- Bartnicki-García, S. 1987. The cell wall: a crucial structure in fungal evolution, pp. 389–403. In Rayner, A.D.M. (ed.), *Evolutionary Biology of the Fungi*, 2nd ed. Cambridge University Press, New York, USA.

- Blumenkrantz, N. and Asboe-Hansen, G.** 1973. New method for quantitative determination of uronic acids. *Anal. Biochem.* **54**, 484–489.
- Bradford, M.M.** 1976. A rapid and sensitive method for the quantitation of microgram quantities of protein utilizing the principle of protein-dye binding. *Anal. Biochem.* **72**, 248–254.
- Braun, P.C. and Calderone, R.A.** 1978. Chitin synthesis in *Candida albicans*: Comparison of yeast and hyphal forms. *J. Bacteriol.* **133**, 1472–1477.
- Chauhan, N.M., Raut, J.S., and Karuppaiyil, S.M.** 2011. Acetaldehyde inhibits the yeast-to-hypha conversion and biofilm formation in *Candida albicans*. *Mycoscience* **52**, 356–360.
- Dos Reis Almeida, F.B., Pigosso, L.L., De Lima Damasio, A.R., Monteiro, V.N., De Almeida Soares, C.M., Silva, R.N., and Roque-Barreira, M.C.** 2014.  $\alpha$ -(1,4)-Amylase, but not  $\alpha$ - and  $\beta$ -(1,3)-glucanases, may be responsible for the impaired growth and morphogenesis of *Paracoccidioides brasiliensis* induced by N-glycosylation inhibition. *Yeast* **31**, 1–11.
- Dow, J.M., Darnall, D.W., and Villa, V.D.** 1983. Two distinct classes of polyuronide from the cell walls of a dimorphic fungus, *Mucor rouxii*. *J. Bacteriol.* **155**, 1088–1093.
- DuBois, M., Gilles, K.A., Hamilton, J.K., Rebers, P.A., and Smith, F.** 1956. Colorimetric method for determination of sugars and related substances. *Anal. Chem.* **28**, 350–356.
- Garron, M.L. and Cygler, M.** 2010. Structural and mechanistic classification of uronic acid-containing polysaccharide lyases. *Glycobiology* **20**, 1547–1573.
- Georgopapadakou, N. and Walsh, T.** 1994. Human mycoses: Drugs and targets for emerging pathogens. *Science* **264**, 371–373.
- Ghormade, V. and Deshpande, M.V.** 2000. Fungal spore germination into yeast or mycelium: Possible implications of dimorphism in evolution and human pathogenesis. *Naturwissenschaften*. **87**, 236–240.
- Hogan, L.H. and Klein, B.S.** 1994. Altered expression of surface  $\alpha$ -1,3-glucan in genetically related strains of *Blastomyces dermatitidis* that differ in virulence. *Infect. Immun.* **62**, 3543–3546.
- Holbrook, E.D. and Rappleye, C.A.** 2008. *Histoplasma capsulatum* pathogenesis: making a lifestyle switch. *Curr. Opin. Microbiol.* **11**, 318–324.
- Hou, L.H., Chen, Y., Ma, C.J., Liu, J., Chen, L.G., and Ma, A.M.** 2011. Effects of environmental factors on dimorphic transition of the jelly mushroom *Tremella fuciformis*. *Cryptogamie Mycol.* **32**, 421–428.
- Kanetsuna, F. and Carbonell, L.M.** 1971. Cell wall composition of the yeastlike and mycelial forms of *Blastomyces dermatitidis*. *J. Bacteriol.* **106**, 946–948.
- Khondkar, P., Aidoo, K.E., and Tester, R.F.** 2002. Sugar profile of extracellular polysaccharides from different *Tremella* species. *Int. J. Food Microbiol.* **79**, 121–129.
- Klein, B.S. and Tebbets, B.** 2007. Dimorphism and virulence in fungi. *Curr. Opin. Microbiol.* **10**, 314–319.
- Klis, F.M., Ram, A.F.J., and Groot, P.W.J.** 2007. A molecular and genomic view of the fungal cell wall, pp. 97–120. In Howard, R. (ed.), *Biology of the Fungal Cell*, 2nd ed. Springer-Verlag, Berlin, Germany.
- Kraus, J., Blaschek, W., Schutz, M., and Franz, G.** 1992. Antitumor activity of cell wall  $\beta$ -1,3/1,6-glucans from *Phytophthora* species. *Planta. Med.* **58**, 39–42.
- Leal, J.A. and Bernabé, M.** 1998. Taxonomic applications of polysaccharides, pp 153–181. In Frisvad, J.C. (ed.), *Chemical Fungal Taxonomy*, Dekker, New York, USA.
- Lee, J.S., Kwon, J.S., Won, D.P., Lee, K.E., Shin, W.C., and Hong, E.K.** 2010. Study on macrophage activation and structural characteristics of purified polysaccharide from the liquid culture broth of *Cordyceps militaris*. *Carbohydr. Polym.* **82**, 982–988.
- Leung, M.Y.K., Fung, K.P., and Choy, Y.M.** 1997. The isolation and characterization of an immunomodulatory and anti-tumor polysaccharide preparation from *Flammulina velutipes*. *Immunopharmacology* **35**, 255–263.
- Li, N.S., Yan, C.Y., Hua, D.H., and Zhang, D.Z.** 2013. Isolation, purification, and structural characterization of a novel polysaccharide from *Ganoderma capense*. *Int. J. Biol. Macromol.* **57**, 285–290.
- Liu, J., Ma, A.M., Sheng, G.H., Chen, L.G., and Xie, B.J.** 2007. Preliminary study on the differences of dimorphic cells in *Tremella fuciformis*. *Microbiol. China* **34**, 53–57.
- Liu, J., Wu, Y., Ma, A.M., and Chen, L.G.** 2008. Research progress of environmental factors and signal transduction pathways of dimorphism in fungi. *Microbiol. China* **35**, 1102–1106.
- Maresca, B. and Kobayashi, G.S.** 1989. Dimorphism in *Histoplasma capsulatum*: A model for the study of cell differentiation in pathogenic fungi. *Microbiol. Rev.* **53**, 186–209.
- Mysyakina, I.S., Bokareva, D.A., Usov, A.I., and Feofilova, E.P.** 2012. Differences in the carbohydrate composition between the yeast-like and mycelial cells of *Mucor hiemalis*. *Microbiology* **81**, 405–408.
- Nadal, M., Garcia-Pedrajas, M.D., and Gold, S.E.** 2008. Dimorphism in fungal plant pathogens. *FEMS Microbiol. Lett.* **284**, 127–134.
- Nemecek, J.C., Wüthrich, M., and Klein, B.S.** 2006. Global control of dimorphism and virulence in fungi. *Science* **312**, 583–588.
- Puccia, R., Vallejo, M.C., Matsuo, A.L., and Longo, L.V.G.** 2011. The *Paracoccidioides* cell wall: past and present layers towards understanding interaction with the host. *Front. Microbiol.* **2**, 257–264.
- Rappleye, C.A., Eissenberg, L.G., and Goldman, W.E.** 2007. *Histoplasma capsulatum*  $\alpha$ -(1,3)-glucan blocks innate immune recognition by the  $\beta$ -glucan receptor. *Proc. Natl. Acad. Sci. USA* **104**, 1366–1370.
- Rappleye, C.A. and Goldman, W.E.** 2006. Defining virulence genes in the dimorphic fungi. *Annu. Rev. Microbiol.* **60**, 281–303.
- San-blas, G., San-blas, F., and Mackenzie, D.W.R.** 1984. Molecular aspects of fungal dimorphism. *Crit. Rev. Microbiol.* **11**, 101–127.
- Sietsma, J.H. and Wessels, J.G.H.** 1994. Apical wall biogenesis, pp. 126–141. In Wessels, J.H. and Meinhardt, F. (eds), *Growth, Differentiation and Sexuality*. Springer, Berlin, Germany.